Blends Based on Copolymers of Methyl Methacrylate with Phenyl Maleimide and Tribromophenyl Maleimide

G. D. Merfeld, K. Chan, and D. R. Paul*

Department of Chemical Engineering and Texas Materials Institute, The University of Texas at Austin, Austin, Texas 78712

Received August 4, 1998

ABSTRACT: The synthesis of methyl methacrylate−phenyl maleimide (MMA−PMI) and methyl methacrylate−tribromophenyl maleimide (MMA−TBPMI) copolymers and the phase behavior of their blends are reported. Copolymer compositions that form miscible binary blends with poly(methyl methacrylate) (PMMA) and polycarbonate (PC) and with copolymers of styrene−acrylonitrile (SAN) and styrene−maleic anhydride (SMA) were established. Repeat unit interaction energies were estimated from isothermal phase boundaries using a binary interaction model and the Flory−Huggins theory. All binary interactions with PMI and TBPMI were found to be endothermic. In general, the interactions with TBPMI are more favorable than with PMI, notwithstanding the interaction with AN where the opposite is true. LCST phase separation was measured for selected blends and compared with predictions based on the Sanchez−Lacombe equation of state.

Introduction

Incorporation of halogen atoms into the repeat units of polymers can lead to improved heat and chemical resistance, permeability, and flame retardancy;[1−3] as a result, these materials are potentially useful components in polymer blends. Further, because halogens are electron-dense groups, their presence can impart local polarization which, in turn, can give rise to favorable molecular interactions with certain polymer repeat units. In fact, it has been proposed that preferential halogen/carbonyl interactions give rise to miscibility in certain blends of halogen-containing polymers with aliphatic polyesters, polymethacrylates, polyacrylates, and polycarbonates.[4−12] In this study, copolymers of methyl methacrylate (MMA) with phenyl maleimide (PMI) and of MMA with tribromophenyl maleimide (TBPMI) are synthesized, characterized, and blended with various polymers including polycarbonate (PC), poly(methyl methacrylate) (PMMA), styrene−acrylonitrile (SAN), and styrene−maleic anhydride (SMA) copolymers. By investigating how the blend phase behavior changes with copolymer composition and modeling those observations with the Flory−Huggins theory and a binary interaction model, it is possible to quantify the interaction energies between repeat unit pairs. Furthermore, comparing the phase behavior and the interaction energies of the brominated and the nonbrominated analogues offers an interesting opportunity to identify structure−miscibility relationships and to isolate the contribution made by the bromine atoms.

Blend Thermodynamics

To model or predict polymer blend phase behavior, it is convenient to begin with the Flory−Huggins formulation[13,14] for the Gibbs free energy of mixing two monodisperse homopolymers A and B

$$\Delta g_{mix} = B\phi_A\phi_B + RT\left[\frac{\rho_A\phi_A \ln \phi_A}{M_A} + \frac{\rho_B\phi_B \ln \phi_B}{M_B}\right] \quad (1)$$

Energetic interactions are described by the van Laar quadratic term where B is the interaction energy density for the binary pair A−B; it is weighted by the probability of A−B contacts which, assuming random mixing, is the product of the volume fractions $\phi_A\phi_B$. For polymer blends to be miscible, not only should the Gibbs free energy of mixing be negative but, additionally, its second derivative with respect to blend composition should be positive to ensure stability against random fluctuations. Evaluating eq 1 at the critical condition for miscibility gives

$$B_{critical} = \left(\sqrt{\frac{\rho_A}{(\bar{M}_W)_A}} + \sqrt{\frac{\rho_B}{(\bar{M}_W)_B}}\right)^2 \quad (2)$$

where polydispersity is treated properly in this expression using weight average molecular weights, $\bar{M}_W$.[15,16] For miscibility, the overall interaction energy B must be more favorable than $B_{critical}$.

The interactions in copolymer blends can be expressed in terms of pairwise interactions between the repeat units using a binary interaction model.[17−19] When a homopolymer (1) and a copolymer (1−2) containing a common repeat unit type are blended, the binary interaction model reduces to

$$B = B_{12}\phi_2^2 \quad (3)$$

where ϕ_2 is the volume fraction of 2 in the copolymer. Regardless of the magnitude of B_{12}, the homopolymer will always be able to tolerate at least some limiting amount of 2 in the copolymer and still maintain miscibility for finite component molecular weights. When the homopolymer (1) and the copolymer (2−3) do not have a common repeat unit type, the interaction energy is given by

$$B = B_{12}\phi_2 + B_{13}\phi_3 - B_{23}\phi_2\phi_3 \quad (4)$$

For a blend of copolymer (1−2) with copolymer (1−3) the result is

10.1021/ma981230p CCC: $18.00
Published on Web 12/29/1998

$$B = B_{12}(\phi_2^2 - \phi_2\phi_3) + B_{13}(\phi_3^2 - \phi_2\phi_3) + B_{23}\phi_2\phi_3 \quad (5)$$

As in eq 4, only three binary interaction energies are needed in this case; however, for a blend of two copolymers where all the repeat units are unique in structure, there are six possible binary interactions, and the model becomes

$$B = B_{13}\phi_1\phi_3 + B_{14}\phi_1\phi_4 + B_{23}\phi_2\phi_3 + B_{24}\phi_2\phi_4 - B_{12}\phi_1\phi_2 - B_{34}\phi_3\phi_4 \quad (6)$$

By combining the Flory−Huggins theory with the appropriate form of the binary interaction model, it is possible to model the isothermal phase behavior of copolymer blends to either extract estimates for unknown binary interaction energies or predict phase behavior when the required binary interaction energies are known. Lower critical solution temperature (LCST) type phase diagrams typically observed in polymer blends cannot be modeled by the Flory−Huggins theory unless the interaction energies are known as a function of temperature. To predict LCST phase separation, it is more appropriate to use an equation of state like the lattice fluid theory of Sanchez and Lacombe.[20−22] The latter is a corresponding states theory referenced to experimentally measured characteristic *PVT* parameters and in which ΔP_{ij} interaction parameters, used instead of the Flory−Huggins B_{ij} parameters, have the distinct advantage of being pure interactions free from compressibility effects. The application of this theory to polymer blends has been demonstrated in detail elsewhere.[23,24]

Synthesis and Characterization of PMI and TBPMI Copolymers. Methyl methacrylate (MMA) was copolymerized with tribromophenyl maleimide (TBPMI) and with phenyl maleimide (PMI). The structures of the maleimide monomers are illustrated in Figure 1. Syntheses of MMA−TBPMI copolymers[25−27] and of MMA−PMI copolymers[28−31] have been reported previously. Methyl methacrylate (Aldrich Chemical Co.) was vacuum distilled to remove inhibitors and kept refrigerated until use. To ensure purity, tribromophenyl maleimide (provided courtesy of AmeriBrom Inc.) was recrystallized from ethanol while phenyl maleimide (Aldrich Chemical Co.) was recrystallized from a (1:1) ethanol:water mixture. The purity of the maleimide monomers was verified by gas chromatography, proton NMR, and elemental analysis. Sharp melting points of 139 and 90 °C were measured for the purified TBPMI and PMI crystals, respectively; these values closely agree with reports in the literature.[25,30] Free radical polymerizations were performed at 60 °C in dioxane using AIBN as the initiator. The reaction times were adjusted to keep conversions at less than 15%, thereby avoiding significant drift in the copolymer compositions. The reactions were quenched in methanol and the copolymers purified by repeated precipitation of a concentrated polymer/tetrahydrofuran solution into methanol. The copolymers were dried under vacuum for several days before characterization.

Tables 1 and 2 summarize the physical properties of the MMA−PMI and MMA−TBPMI copolymers, respectively. Each copolymer is described by its monomer feed composition listed in parentheses; for example, MMA−PMI (90−10) was made from a monomer feed containing 90 wt % MMA and 10 wt % PMI. The numerical suffix attached to each copolymer acronym corresponds to the weight percent of PMI or TBPMI charged to the reactor for synthesis; the actual weight percent incorporated into each copolymer is listed in the table. These were evaluated by elemental analysis by Atlantic Microlabs of Norcross, GA; TBPMI copolymers were analyzed for bromine content while PMI copolymers were analyzed for nitrogen content.

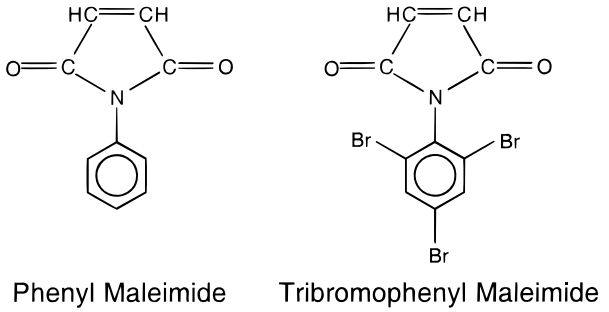

Figure 1. Maleimide monomer structures.

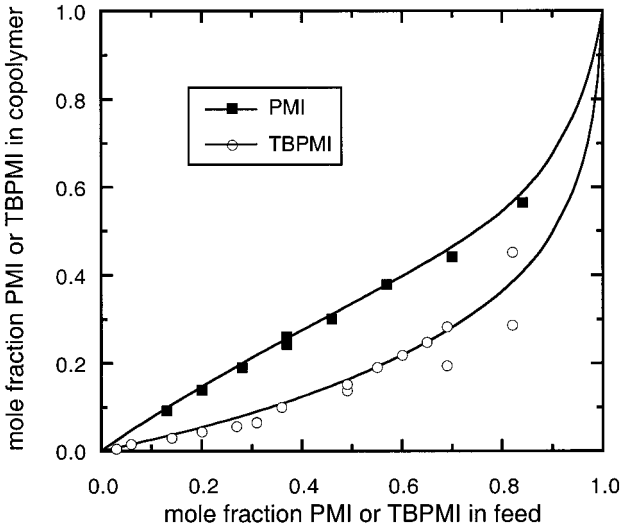

Figure 2. Copolymer versus monomer feed composition for the free radical polymerization of MMA with PMI and with TBPMI carried out to conversions of less than 15 wt %. From the fits to the data shown, reactivity ratios given in the text were estimated.

A plot of PMI or TBPMI mole fraction in the reaction feed versus that actually incorporated into the copolymer is shown in Figure 2. From the curve fits shown, reactivity ratios were estimated for both copolymer families. For MMA−PMI copolymers, values of $r_{PMI} = 0.14$ and $r_{MMA} = 1.25$ were determined and are in line with estimates of $r_{PMI} = 0.183$ and $r_{MMA} = 1.022$ reported by Choudhary et al.[29] Values of $r_{TBPMI} = 0.04$ and $r_{MMA} = 4.20$ were calculated for MMA−TBPMI copolymers and compare favorably with values of $r_{TBPMI} = 0.037$ and $r_{MMA} = 4.32$ reported by Janovic et al.[25] The self-polymerization of either PMI or TBPMI is highly unfavorable as evidenced by these reactivity ratios. Hence, it became increasingly difficult to carry out polymerizations as the content of the maleimide monomers increased so homopolymers of TBPMI or of PMI were not prepared.

Copolymer molecular weights were evaluated by gel permeation chromatography (GPC) calibrated with polystyrene standards. In both copolymer families, the molecular weights were relatively close to a targeted weight average value of 100 000 g/mol, with the largest deviations occurring in copolymers containing the high-

Table 1. MMA−PMI Copolymers

copolymer	acronym	wt % PMI[a]	$\bar{M}_w$[b]	$\bar{M}_n$[b]	T_g (°C) onset	density (g/cm^3)[c]	5% wt loss temp (°C)[d]
MMA−PMI (90−10)	PMI10	7.5	92 000	65 000	128		319
MMA−PMI (80−20)	PMI20	14.8	76 000	48 000	132	1.217	368
MMA−PMI (70−30)	PMI30	21.7	82 000	49 000	139	1.233	378
MMA−PMI (60−40)	PMI40	28.8	95 000	56 000	147	1.234	388
MMA−PMI (50−50)	PMI50	35.5	95 000	58 000	156	1.252	398
MMA−PMI (40−60)	PMI60	42.5	92 000	55 000	168	1.259	400
MMA−PMI (30−70)	PMI70	51.1	99 000	57 000	178	1.263	410
MMA−PMI (20−80)	PMI80	57.6	62 000	34 000	196	1.270	424
MMA−PMI (10−90)	PMI90	69.0	37 000	34 000	224	1.285	424

[a] Determined by elemental analysis for nitrogen. [b] Determined by GPC analysis using PS standards. [c] Measured in a density gradient column at 25 °C. [d] Determined by TGA analysis at a scan rate of 40 °C/min.

Table 2. MMA−TBPMI Copolymers

copolymer	acronym	wt % TBPMI[a]	$\bar{M}_w$[b]	$\bar{M}_n$[b]	T_g (°C) onset	density (g/cm^3)[c]	5% wt loss temp (°C)[d]
MMA−PMI (90−10)	TBPMI10	1.7	106 000	75 000	115	1.216	286
MMA−PMI (80−20)	TBPMI20	5.8	92 000	62 000	116	1.233	288
MMA−PMI (60−40)	TBPMI40	10.9	92 000	64 000	122	1.258	311
MMA−PMI (50−50)	TBPMI50	15.8	85 000	56 000	127	1.286	316
MMA−PMI (40−60)	TBPMI60	19.4	87 000	58 000	131	1.306	328
MMA−PMI (35−65)	TBPMI65-A	22.1	85 000	59 000	140	1.328	
MMA−PMI (35−65)	TBPMI65	22.3	55 000	40 000	141		
MMA−PMI (30−70)	TBPMI70	31.2	87 000	47 000	140	1.404	352
MMA−PMI (20−80)	TBPMI80	39.6	89 000	54 000	158	1.439	387
MMA−PMI (20−80)	TBPMI80-A	42.6	53 000	32 000	158	1.465	
MMA−PMI (10−90)	TBPMI90	49.6	62 000	37 000	180		399
MMA−PMI (5−95)	TBPMI95	62.2	49 000	30 000	208		420

[a] Determined by elemental analysis for nitrogen. [b] Determined by GPC analysis using PS standards. [c] Measured in a density gradient column at 25 °C. [d] Determined by TGA analysis at a scan rate of 40 °C/min.

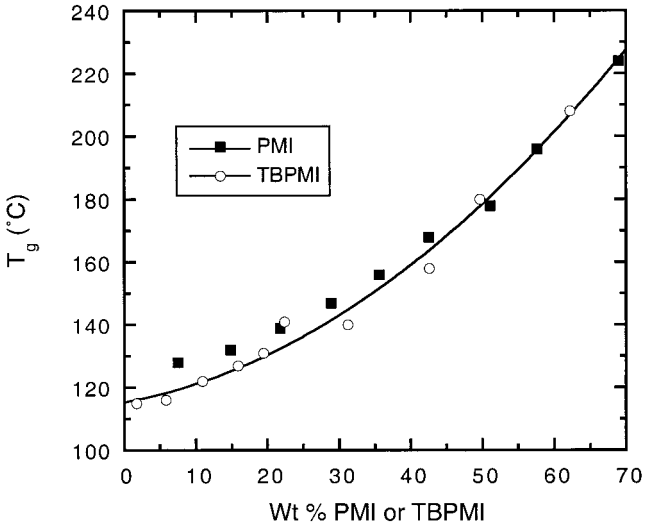

Figure 3. Dependence of glass transition temperature on MMA−PMI and MMA−TBPMI copolymer composition. The effect of bromine substitution appears to be negligible.

est amounts of TBPMI or PMI. Lower molecular weight versions of MMA−TBPMI (35−65) and (20−80) were prepared and used in selected blend studies; these are indicated in Table 2 by the acronyms TBPMI65-A and TBPMI80-A. Glass transition temperatures were measured by differential scanning calorimetry (DSC) using a Perkin-Elmer DSC-7 at a scan rate of 20 °C/min. Two scans were performed: the first to erase thermal history and the second to evaluate thermal characteristics. The glass transitions reported in Tables 1 and 2 were evaluated by the onset method. Figure 3 shows that these values are strong, continuous functions of the TBPMI or PMI content, with the presence of bromine in TBPMI copolymers having a negligible effect on the glass transition compared to the case of PMI copolymers. The differences between PMI and TBPMI copolymer densities are significant, however, owing to the high molecular mass of bromine. Measurements made in a density gradient column at 25 °C using $ZnCl_2$ solutions are included in Tables 1 and 2.

Additionally, the copolymers were tested for thermal stability by thermogravimetric analysis (TGA) in a Perkin-Elmer TGA-7. Using a scan rate of 40 °C/min, the temperature at which the samples lost 5% of their total weight was determined. These temperatures are reported in Tables 1 and 2. Like the glass transition behavior, there is an increase in thermal stability as either TBPMI or PMI content increases in the copolymer; however, MMA−PMI copolymers have a slightly higher degradation temperature compared to MMA−TBPMI copolymers of comparable maleimide content. For reference, PMMA homopolymers with and without ethyl acrylate to prevent chain unzipping were also studied. All the copolymers synthesized here were more thermally stable than the pure PMMA, while all except MMA−TBPMI copolymers containing less than 6 wt % TBPMI were more stable than the PMMA containing approximately 5 wt % ethyl acrylate.

Finally, the *PVT* properties of selected copolymers were measured in a Gnomix *PVT* apparatus. These results are presented later in a discussion of the equation-of-state prediction of phase separation.

Blend Preparation and Evaluation

Blends (all 50/50 by weight) were prepared by casting from a common solvent, tetrahydrofuran, onto glass slides heated to 60 °C. Evaporation of the solvent took less than 5 min and produced smooth films. These were held an additional 15 min on the heated slides and then transferred to a vacuum oven where the temperature

was gradually increased to 150 or 170 °C. After annealing for 36 h or more in the vacuum oven, the samples were removed. Visual assessments of blend miscibility were made both before and after the annealing treatment. Any change upon annealing could suggest that the solvent preparation technique may have trapped blends in a nonequilibrium state; however, in all cases the observations did not change. As a second evaluation of blend miscibility, each sample was analyzed by DSC. Since visual techniques fail when the refractive indices of the blend components are nearly matched and DSC techniques fail when the glass transition temperatures of the components are indiscernibly close, a combination of both methods was employed to confirm phase behavior. In situations where only optical observations could be used, a more quantitative analysis was possible with the use of light scattering. The apparatus used for this work is described in detail elsewhere.[32] For these measurements, the intensity of static V_v scattering of a HeNe laser (632.8 nm) was collected for wavevectors between 1.8 and 10.6 $Å^{-1}$. For each sample, the scattered intensity was integrated over the collected wavevectors and then normalized for the film thickness. A relative comparison of these values was used to assist in optical assessment of phase behavior.

Phase separation temperatures, all of the LCST type, were bracketed below temperatures where a change from clear to cloudy or from one glass transition to two was recorded and above temperatures where extended annealing times failed to induce phase separation.[33] When possible, rehomogenization of phase-separated blends was used to confirm reversibility of the process. Prohibitively slow rates of diffusion and thermal degradation, however, prevented verification of reversibility in some cases.

Blends with Poly(methyl methacrylate)

Although the interaction between methyl methacrylate and either of the maleimide repeat units studied here is likely to be unfavorable (as a general rule, most repeat unit pair interactions are), copolymers of MMA with PMI or TBPMI should be miscible with PMMA up to some limiting copolymer composition. Knowledge of how much PMI or TBPMI can be tolerated before the miscibility limit is reached can be used to quantify $B_{MMA/PMI}$ or $B_{MMA/TBPMI}$. Only the discrete copolymer compositions listed in Tables 1 and 2 are available for such a study, however, and the associated binary interactions can be determined, at best, as falling between estimates calculated using the upper and lower copolymer compositions that bracket the miscibility border. As has been demonstrated elsewhere,[24] more refined estimates can be made when the homopolymer is available over a range of molecular weights. Lowering the PMMA molecular weight should predictably expand the miscibility to higher copolymer compositions owing to the added entropic contribution to mixing. The nearly monodisperse poly(methyl methacrylate) homopolymers listed in Table 3 (sold commercially as standards) are ideally suited for such studies. By combining eqs 2 and 3, the following expression is obtained

$$\phi_{PMI} = \sqrt{\frac{RT}{2B_{MMA/PMI}}}\left(\sqrt{\frac{\rho_{PMMA}}{(\bar{M}_W)_{PMMA}}} + \sqrt{\frac{\rho_{MMA/PMI}}{(\bar{M}_W)_{MMA/PMI}}}\right) \quad (7)$$

Table 3. Homopolymers Used in This Study

polymer	$\bar{M}_w$[b]	$\bar{M}_n$[b]	T_g (°C) onset
PMMA	105 000	42 700	115
PMMA	73 900	69 100	119
PMMA	60 000	56 000	126
PMMA	33 500	31 300	125
PMMA	20 300	18 300	125
PMMA	10 550	9 500	108
PMMA	4 250	4 000	99
PMMA	2 400	2 200	77
PMMA	1 400	1 200	
PC	38 000	14 600	146
PC	29 900	10 800	142
PC	13 500	6 200	138

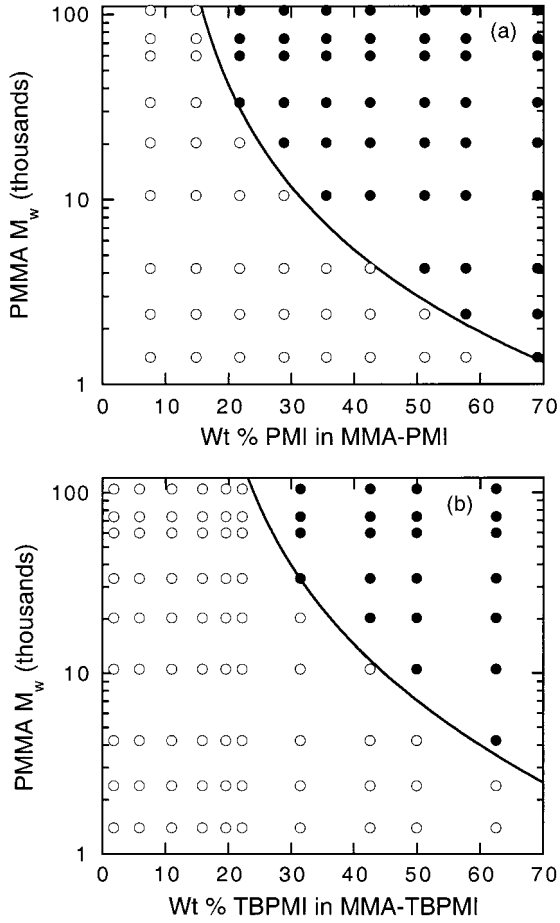

Figure 4. Isothermal miscibility at 150 °C for 50/50 blends of PMMA of varying molecular weights with (a) MMA−PMI copolymers and (b) MMA−TBPMI copolymers. Open circles indicate miscible blends while closed circles indicate immiscible blends. The curves shown were predicted using binary interaction energies of $B_{MMA/PMI} = 1.0$ and $B_{MMA/TBPMI} = 0.8$ cal/cm^3.

Thus, a plot of ϕ_{PMI} versus $(\rho_{PMMA}/(\bar{M}_W)_{PMMA})^{1/2}$ will allow evaluation of $B_{MMA/PMI}$ from the slope of a line drawn to separate miscible from immiscible blends. The analogous study for PMMA/MMA−TBPMI blends will yield an estimate for $B_{MMA/TBPMI}$.

The phase behavior at 150 °C for blends of MMA−PMI and MMA−TBPMI copolymers with poly(methyl methacrylates) of varying molecular weights is summarized in Figure 4. The region of miscibility with the brominated copolymers is larger than that of its nonbrominated analogues. These results are plotted according to eq 7 in Figure 5; from the slope the following estimates were obtained $B_{MMA/PMI} = 1.0 \pm 0.1$ and

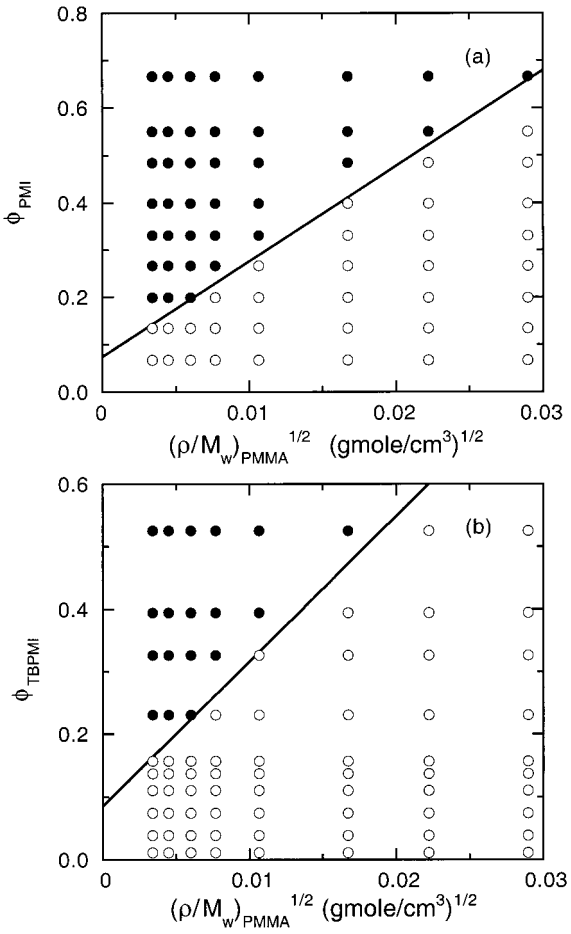

Figure 5. Graphical analysis of data in Figure 4 according to eq 7. From the slope of the lines drawn separating miscible and immiscible blends estimates of (a) $B_{MMA/PMI} = 1.0 \pm 0.1$ and of (b) $B_{MMA/TBPMI} = 0.8 \pm 0.05$ cal/cm^3 were obtained.

$B_{MMA/TBPMI} = 0.8 \pm 0.05$ cal/cm^3. The uncertainties assigned to these values reflect acceptable variation in the fit of the model to the data. Calculations based on these estimates predict that a commercial PMMA ($\bar{M}_W$ = 100 000 g/mol) would be miscible with MMA−PMI copolymers containing approximately 15 wt % and less PMI and with MMA−TBPMI copolymers containing about 22 wt % and less TBPMI.

Blends with Polycarbonate

Blends of PC and PMMA with typical commercial molecular weights are immiscible, but certain copolymers of MMA have been demonstrated to be miscible with PC. For example, Nishimoto et al. studied the phase behavior of PC with methacrylate-based copolymers and found miscibility in MMA copolymers with cyclohexyl methacrylate and with phenyl methacrylate over certain copolymer composition ranges.[34] Ohnaga et al. reported PC miscibility with a terpolymer of MMA, cyclohexyl methacrylate, and 2,4,6-tribromophenyl methacrylate.[35] Similarly, copolymers of MMA with phenyl maleimide repeat units may show miscibility with PC while also, in the case of the brominated phenyl maleimide, imparting flame retardance. Blends of PC with MMA−PMI copolymers have been claimed in patents,[36,37] and a limited investigation of these blends has been reported in the literature.[38] A thorough investigation of how blend phase behavior is affected by concurrent changes in copolymer composition and PC molecular weight can be used to quantify unknown repeat unit interactions. The PC homopolymers used in this study are listed in Table 3.

Special consideration was necessary in preparing these blends since polycarbonates can crystallize during solvent casting, especially lower molecular weight polycarbonates. This was of particular concern here because the glass transition of PC and many of the copolymers was too close to discern by DSC, and therefore, evaluation of miscibility relied on visual/optical assessments. To avoid PC crystallization, blends were prepared by precipitating dilute THF solutions of the polymers into methanol. The recovered precipitate was dried under vacuum at low temperatures for several days and then melted between glass slides at 240 °C to form smooth blend films free of PC crystallization. PC/MMA−TBPMI blends prepared by this method showed a well-defined window of miscibility, but all PC/MMA−PMI blends were found to be immiscible at 240 °C. Without at least some miscibility, it would not be possible to make an evaluation of the PC/PMI interaction energy. Therefore, an alternative approach, discussed below, was used to study the PC/MMA−PMI blends.

Although PC and PMMA with commercially useful molecular weights are immiscible, Callaghan et al. showed that their mixtures become miscible by lowering both of the component molecular weights sufficiently.[39] This is because even though the PC/MMA binary interaction energy is unfavorable, it is small enough that the increase in entropy attributed to lowering polymer molecular weight can shift the thermodynamic balance toward miscibility. This study produced a reliable estimate of $\Delta P^*_{PC/MMA} = 0.0043$ cal/cm^3. Further, an equation-of-state relationship allowed conversion of this ideally temperature and composition invariant bare interaction energy to a temperature-dependent Flory−Huggins parameter, i.e., $B_{PC/MMA} = -0.04 + (2.7 \times 10^{-4})T$ where T is the temperature in kelvin.[39] At 240 °C this gives $B_{PC/MMA} = 0.100$ while at 150 °C $B_{PC/MMA} = 0.075$ cal/cm^3 is predicted. Calculations based on these interaction energies suggest that PMMA ($\bar{M}_W = 100\,000$ g/mol) should be miscible with the lowest molecular weight PC listed in Table 3. Therefore, the best opportunity to observe miscibility of PC with MMA−PMI copolymers is at low temperatures with the lowest PC molecular weight and with MMA−PMI copolymers that contain the smallest amount of PMI. With this insight, PC/MMA−PMI blends were further investigated at 150 °C using a solvent casting procedure that increased the rate of solvent evaporation in order to minimize PC crystallization. Visual observations identified a limited region of miscibility in these blends.

The results of blending PC with MMA−PMI and with MMA−TBPMI copolymers using the methods described above are shown in Figure 6. These plots summarize the effect of molecular weight and copolymer composition on phase behavior. To enable consideration of the molecular weights of the PC and copolymer simultaneously, $B_{critical}$, calculated using eq 2, is plotted along the ordinate. For a given copolymer, three $B_{critical}$ values are plotted corresponding to blends with each of the three PC molecular weights. As PC molecular weight decreases, $B_{critical}$ increases. For blends with a given PC, the $B_{critical}$ tends to increase as more PMI or TBPMI is incorporated into the copolymer owing to the reduction in copolymer molecular weight documented in Table 2. It must be emphasized that a direct comparison between

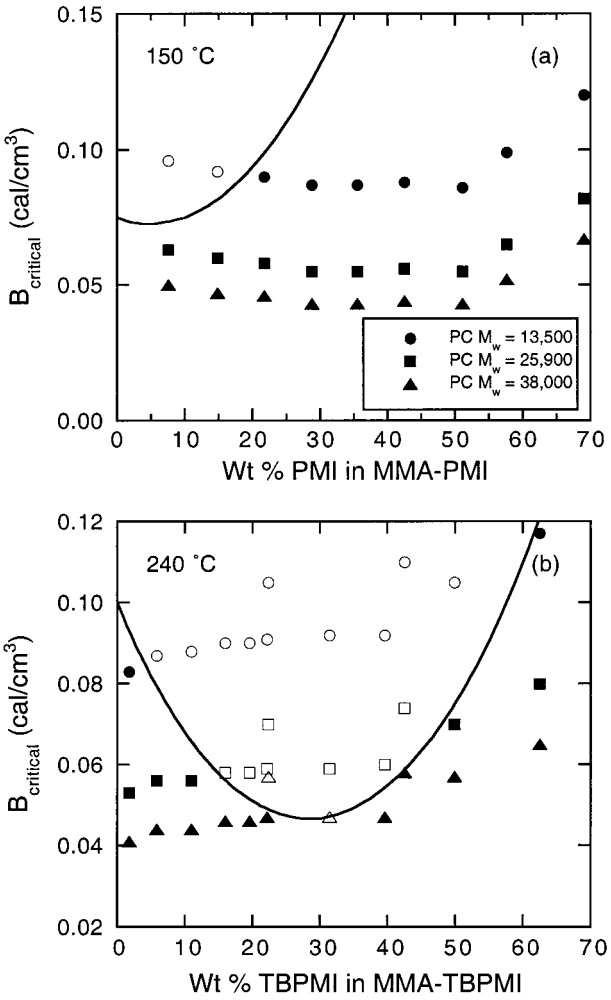

Figure 6. Isothermal phase behavior for 50/50 blends of PC with (a) MMA−PMI copolymers at 150 °C and (b) MMA−TBPMI copolymers at 240 °C. The effect of molecular weight on miscibility, summarized in terms of $B_{critical}$ values calculated using eq 2, is considered as a function of copolymer composition. Open and closed symbols represent blends assessed to be miscible and immiscible, respectively, with the three PC molecular weights indicated. Equation 4 and the following interaction energies, $B_{PC/MMA} = 0.075$ at 150 °C, $B_{PC/MMA} = 0.10$ at 240 °C, $B_{MMA/PMI} = 1.00$, $B_{MMA/TBPMI} = 0.82$, $B_{PC/PMI} = 0.97$, and $B_{PC/TBPMI} = 0.50$ cal/cm^3, were used to calculate the solid lines shown.

parts a and b of Figure 6 cannot be made because the PC/MMA−PMI phase behavior was measured at 150 °C while that for PC/MMA−TBPMI blends was measured at 240 °C. Nonetheless, in general, the opportunity for miscibility with the brominated copolymers is greater and expands significantly as PC molecular weight is lowered.

Static light scattering, described earlier, was a vital tool for establishing the windows of miscibility shown in Figure 6. In these systems, the region of miscibility happens to coincide with blend compositions where the glass transition behavior of the components cannot be distinguished; therefore, assessment of miscibility was based on visual/optical evaluations. Visual observations alone would have been too subjective, but when combined with the light scattering measurements, the regions of miscibility were identified with confidence. Figure 7 summarizes the static light scattering measurements for PC/MMA−TBPMI blends. The labels on the *x*-axis indicate the MMA−TBPMI copolymer composition in terms of the weight percent TBPMI used in the monomer feed; this corresponds to the acronym suffix assigned in Table 2. For presentation purposes, the lower molecular weight versions of MMA−TBPMI (TBPMI65-A and TBPMI80-A) have been omitted. The heavy solid lines included in the graphs mark where the distinction between miscible and immiscible was drawn; blends with a normalized scattering intensity below this line were recorded as miscible while those above as immiscible. The evaluation line in the center plot for blends with PC $\bar{M}_W = 29\,900$ is drawn with a slope that differentiates blends with TBPMI50 as miscible and with TBPMI90 as immiscible even though they have nearly the same normalized scattering intensity. This distinction is appropriate, however, because it considers the decease in the index of refraction difference (i.e., phase contrast) between immiscible phases as the TBPMI content increases in the copolymer.

At the boundary that separates miscible and immiscible blends, the $B_{critical}$ plotted in Figure 6a,b must exactly balance the energetic contribution to mixing given by the binary interaction model in eq 4. For both blend systems, three binary interaction energies are needed to describe this boundary; however, two of these are known already for each system. The estimates of $B_{PC/MMA} = 0.075$ at 150 °C and $B_{PC/MMA} = 0.10$ cal/cm^3 at 240 °C discussed previously can be used here with confidence; likewise, from the earlier study of blends with PMMA homopolymers estimates of $B_{MMA/PMI} = 1.0 \pm 0.1$ and $B_{MMA/TBPMI} = 0.8 \pm 0.5$ cal/cm^3 are also known. The remaining binary interaction energies, $B_{PC/PMI}$ and $B_{PC/TBPMI}$, can be estimated by fitting the binary interaction model to the data. The curves shown in Figure 6 represent the best fit of the model to the data from which values of $B_{PC/PMI} = 1.00 \pm 0.15$ and $B_{PC/TBPMI} = 0.50 \pm 0.05$ cal/cm^3 were obtained. Uncertainties reported with these values were estimated by varying the two known parameters within their confidence limits and noting how much the last parameter had to be adjusted to maintain a reasonable fit to the data. These results show that the PC interaction with the brominated copolymers is considerably more favorable than with their nonbrominated analogues.

From a practical perspective, it is useful to discuss which of these blends could be melt processed without phase separation when the components have typical commercial molecular weights. The methyl methacrylate copolymers studied here all have weight-average molecular weights in the neighborhood of 100 000, typical for commercial PMMA. The PC molecular weights investigated are representative of useful production grades; the higher molecular weight, lower melt flow index, polycarbonates find use in extrusion applications, the midrange materials in injection molded products, and the lowest molecular weights in optical quality parts where the high melt flow index helps to minimize undesired birefringence. Melt processing temperature varies with PC molecular weight and flow requirements, but in general, temperatures of greater than 200 °C are necessary. Thus, the miscible blends of MMA−PMI copolymers with PC ($\bar{M}_W = 13\,500$) at 150 °C shown in Figure 6a would not be single phase when prepared by melting processing because phase separation occurs at temperatures of less than 180 °C. On the other hand, all the miscible MMA−TBPMI copolymer blends with PC identified in Figure 6b could be melt processed at temperatures of 240 °C and less. The approximate

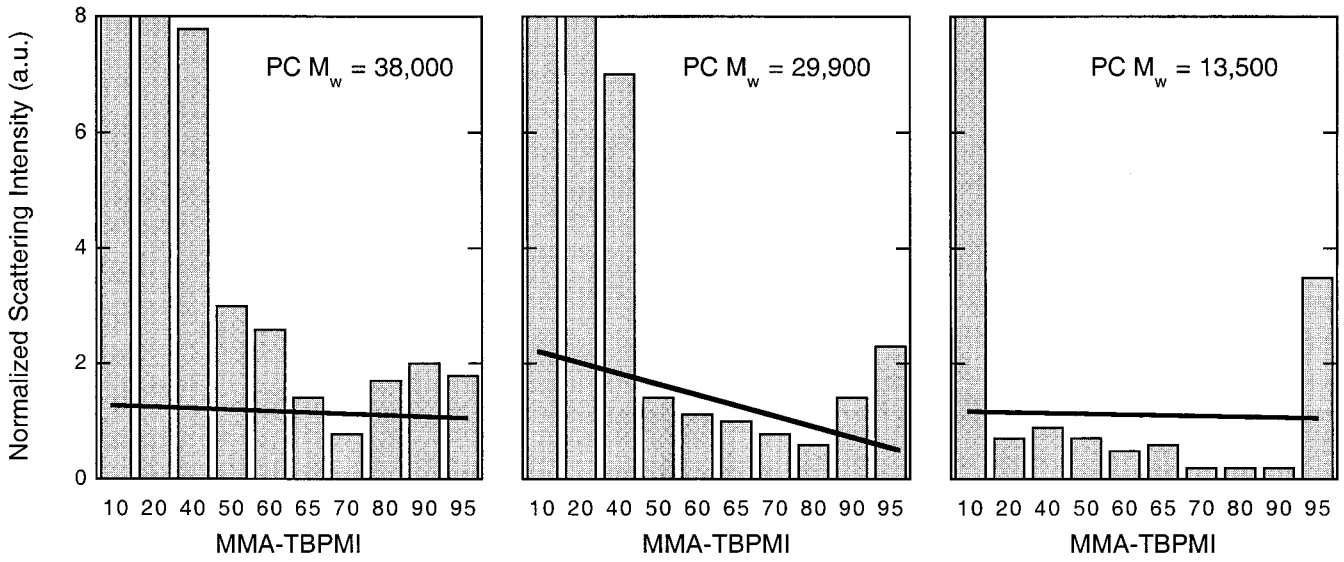

Figure 7. Thickness normalized static light scattering from PC/MMA−TBPMI blends integrated for wavevectors between 1.8 and 10.6 $Å^{-1}$. Combined with visual and phase separation observations, these results were used to identify the region of miscibility shown in Figure 6b.

Table 4. Comparison of Experimentally Measured and Predicted Phase Separation Temperatures (°C)

blend	expt	Sanchez−Lacombe	blend	expt	Sanchez−Lacombe
PC13.5K/PMI10	175	275	PC25.9K/TBPMI65-A	260−270	230
PC13.5K/PMI20	170	185	PC25.9K/TBPMI65	250−260	205
PC13.5K/TBPMI20	240−250	290	PC25.9K/TBPMI70	270−280	215
PC13.5K/TBPMI40	280−290	310	PC25.9K/TBPMI80	260−270	210
PC13.5K/TBPMI90	270−280	240	PC25.9K/TBPMI80-A	250−260	235
PC25.9K/TBPMI40	<240	135	PC25.9K/TBPMI90	<240	155
PC25.9K/TBPMI50	245−255	185	PC38K/TBPMI90	270−280	185
PC25.9K/TBPMI60	250−260	200			

miscible region for MMA−TBPMI copolymers would be between 25 and 35 wt % TBPMI for PC with $\bar{M}_W$ = 38 000, between 15 and 40 wt % TBPMI for PC with $\bar{M}_W$ = 25 900, and between 5 and 50 wt % for PC with $\bar{M}_W$ = 13 500. Use of higher processing temperatures than 240 °C would reduce these windows of miscibility according to the phase separation temperatures reported in Table 4.

All miscible PC blends were studied for phase separation on heating, and the results are summarized in Table 4. Blends that did not phase separate prior to thermal degradation (temperatures greater than 300 °C) are omitted from the table. As expected, the two PC/MMA−PMI blends miscible at 150 °C phase separated before the 240 °C melting mixing temperature where they were found previously to be immiscible, while several PC/MMA−TBPMI blends lying nearest the miscibility boundary showed phase separation at temperatures less than 300 °C. The phase separation temperatures tend to increase as the energetics of the blend become more favorable and as the PC molecular weight is lowered.

Using the binary interaction energies evaluated above in the isothermal analysis, it is possible to make an equation-of-state prediction of phase separation temperatures. This involves converting each B_{ij} to a corresponding ΔP_{ij} and solving the Sanchez−Lacombe equation of state under the thermodynamic constraints of the spinodal phase condition. This procedure has been explained in detail elsewhere.[24] To perform these calculations, it is first necessary to experimentally measure the *PVT* properties of the copolymers and then fit the Sanchez−Lacombe equation of state to the data to extract estimates for the characteristic *PVT* parameters. Figure 8 summarizes the results of these measurements and calculations for selected MMA−PMI and MMA−TBPMI copolymers using *PVT* data collected for a pressure range of 0−50 MPa. The error bars on the data indicate uncertainty in their values attributed to the inability of the equation of state to exactly fit the *PVT* data. They do not include experimental error arising from the *PVT* measurements themselves. It should be noted that *T** values for the two copolymer families do not converge at PS because the evaluations were performed over different temperature ranges. Linear regressions to the parameters as a function of copolymer composition are shown, from which extrapolations to the pure homopolymers of PMI and TBPMI were made. The Sanchez−Lacombe characteristic parameters determined for the latter are listed in Table 5. Also included in Table 5 are characteristic parameters previously reported for PC and PMMA homopolymers.[39]

With this information, spinodal phase separation temperatures were predicted and are included in Table 4 for comparison with the experimental values. Although the predicted temperatures deviate from the measured values, their rough magnitude and how they change with copolymer composition are fairly consistent with the observations. Uncertainty in the binary interaction energies was found to affect the predictions by as much as ±25 °C. Upon considering other sources of error that include *PVT* property measurements, the fit of the equation of state to the *PVT* data, and the extrapolation of copolymer characteristic parameters, the relative agreement found here between experiment and theory is notable.

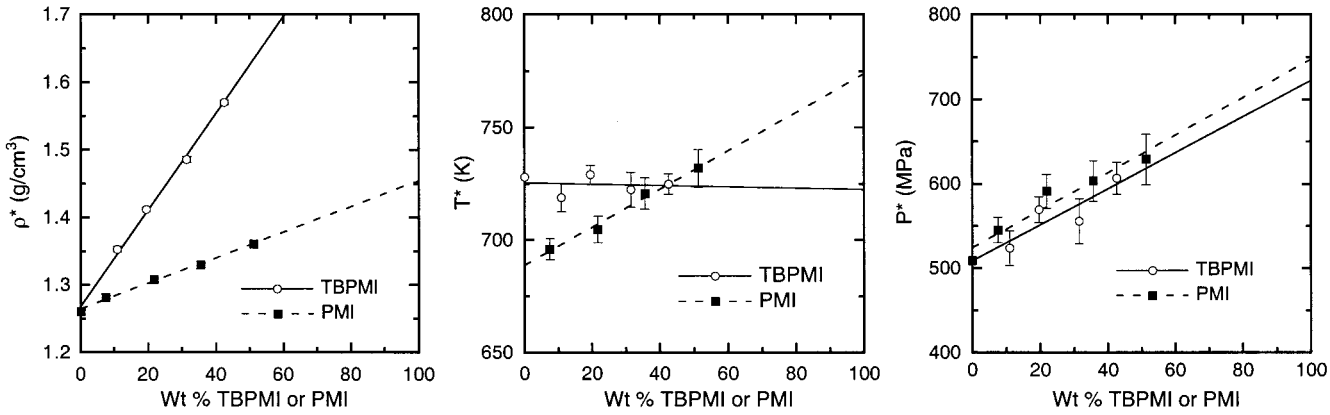

Figure 8. Plots of ρ^*, T^*, and P^* characteristic parameters versus copolymer composition calculated by regression of the Sanchez–Lacombe equation of state onto *PVT* properties measured for MMA–PMI and MMA–TBPMI copolymers. The pure component parameters for PMI and TBPMI obtained by the extrapolations shown are listed in Table 5.

Table 5. Sanchez–Lacombe Characteristic Parameters

repeat unit type	P^* (MPa)	T^* (K)	ρ^* (g/cm³)	temp range (°C)	ref
PC	496	802	1.276	210–270	39
PMMA	509	742	1.256	220–270	39
PMI[a]	747	774	1.455	170–220	this work
TBPMI[a]	722	724	1.984	150–220	this work

[a] Based on an extrapolation of MMA–PMI and MMA–TBPMI copolymer characteristic parameters.

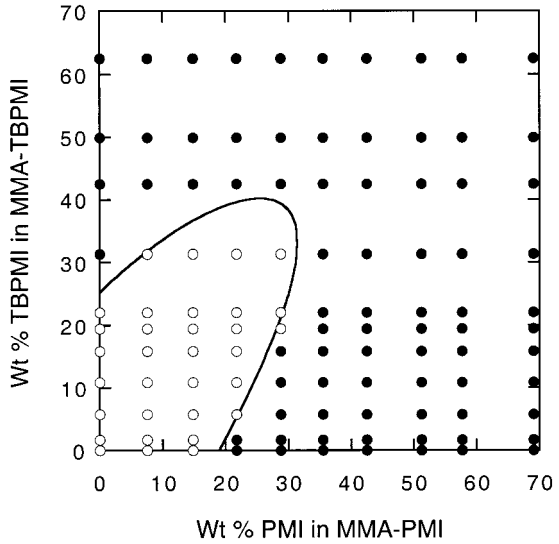

Figure 9. Isothermal miscibility map at 150 °C for 50/50 copolymer/copolymer blends of MMA–PMI and MMA–TBPMI copolymers: (○) miscible and (●) immiscible. The fit of the binary interaction model shown provides an estimate of $B_{MMA/TBPMI} = 0.35 \pm 0.05$ cal/cm³.

MMA–PMI/MMA–TBPMI Blends

Since MMA–PMI and MMA–TBPMI copolymers are both based on methyl methacrylate, it is expected that blends of these copolymers with one another should demonstrate at least some miscibility while the copolymer compositions are close to that of pure PMMA. Experimentally, this proved to be true at 150 °C with the results summarized in Figure 9. Only three binary interaction energies are needed to describe this system, namely $B_{MMA/PMI}$, $B_{MMA/TBPMI}$, and $B_{PMI/TBPMI}$. Estimates for the interactions with MMA were made previously in the study of the copolymer blends with PMMA; in fact, the phase behavior along the axes in Figure 9 is a product of that work. The remaining PMI/TBPMI interaction can be estimated by fitting the binary interaction model given by eq 5 to the isothermal miscibility map. Before this can be performed, though, an estimate for the entropic contribution to mixing must be made. Ideally, the molecular weights of all the copolymers should be identical so that $B_{critical}$ is the same for all blends in the diagram. For this system of blends, the molecular weights are nevertheless roughly similar, and to a good approximation a constant $B_{critical}$ of 0.028 cal/cm³ can be assumed. This is an average value for blends that fall along the miscibility boundary.

An optimized fit of the data, shown as the curve in Figure 9, was calculated using the following set of binary interaction energies: $B_{MMA/PMI} = 0.93$, $B_{MMA/TBPMI} = 0.85$, and $B_{PMI/TBPMI} = 0.35$ cal/cm³. These interactions with MMA fall within the confidence limits established earlier. To evaluate confidence limits for this estimate of $B_{PMI/TBPMI}$, each of the known interaction energies were varied within their own confidence limits while the PMI/TBPMI interaction was adjusted until a reasonable representation of the data was obtained. Good agreement of the model with the data was always possible using values that fall within the range $B_{PMI/TBPMI} = 0.35 \pm 0.05$ cal/cm³.

Blends with Styrenic Copolymers

MMA–PMI and MMA–TBPMI copolymers were blended with both styrene–acrylonitrile (SAN) and styrene–maleic anhydride (SMA) copolymers. Limited miscibility of MMA–PMI with SAN and SMA copolymers has been reported previously in the scientific and patent literature.[40–43] The physical properties of the styrenic copolymers used in this study are summarized in Table 6 where the numerical part of the acronym indicates the weight percent AN or MA in the copolymer. These materials have been described in more detail in previous studies.[44–47] Isothermal miscibility maps measured after annealing at 150 °C are summarized in the four plots of Figure 10. In each plot, when the weight percent PMI or TBPMI is zero, the ordinate corresponds to blends of PMMA with either SAN or SMA. From reports in the literature, these blends are known to be miscible over a limited range of copolymer compositions. For PMMA/SAN blends, the miscibility range is approximately 12–30 wt % AN.[44] For PMMA/SMA blends, the miscibility range is slightly larger, approximately 10–35 wt % MA.[46] Although PMMA provides a common reference for SAN blends in Figure 10a,b and for SMA blends in Figure 10c,d, very differently shaped regions

Table 6. Styrenic Copolymers

copolymer	$\bar{M}_w$	$\bar{M}_n$	T_g (°C) onset
Poly(styrene−acrylonitrile)			
SAN3.8	204 000	93 000	
SAN5.5	212 000		106
SAN6.3	343 000	121 000	104
SAN10	195 600	94 700	104
SAN12.9	151 400	68 300	
SAN15.2	197 000		105
SAN19.5	178 000	88 120	104
SAN25	152 000	77 000	107
SAN28.4	143 800	52 900	111
SAN30	160 000	81 000	109
SAN33	146 000	68 000	112
SAN40	122 000	61 000	113
Poly(styrene−maleic anhydride)			
SMA2	320 000	183 000	105
SMA4.7	179 000	94 000	106
SMA6	273 000	152 000	110
SMA8	200 000	100 000	115
SMA10.1			
SMA14	178 000	92 000	125
SMA18.1	260 000	92 000	135
SMA25	252 000	69 700	149
SMA33			155
SMA47			147
SMA50			

of miscibility were measured as the brominated and the nonbrominated phenyl maleimide content increased in the copolymers.

In general, the size of the miscibility region appears to become larger or at least shift when the phenyl maleimide repeat units are substituted with bromine. This is especially evident for blends with the SMA copolymers; compare parts c and d of Figure 10. This is the same trend observed in blends with PMMA and with PC in which the brominated analogues demonstrated a greater degree of miscibility compared to their nonbrominated counterparts. To quantify this effect in terms of interaction energies, the binary interaction model given by eq 6 was fitted to the miscibility maps.

Because there are four different repeat units in each of these blends, a total of six binary interactions are needed to describe each region of miscibility. Additionally, an average $B_{critical}$ representative of blends lying along the miscibility border must be estimated. After accounting for interaction energies determined earlier in this work and reported in studies elsewhere, only two binary interaction energies for each map are yet undetermined. Moreover, each unknown interaction energy is present in two of the four blend systems shown in Figure 10 such that, collectively, there are six unknown parameters that must be estimated for the four miscibility maps. Rather than optimizing the fit to each diagram individually, an alternative approach is to develop a common set of parameters that produce a consistently good fit for all the maps. Examining the problem in this manner reduces the number of unknowns extracted from each map and should improve the overall quality and "universality" of the estimated interactions.

Before presenting the results of the fitting procedure, it is necessary to first introduce the interaction energies determined elsewhere. These are the interactions that exist between each of the possible pairings of styrene, methyl methacrylate, acrylonitrile, and maleic anhydride, with the exception of the MA/AN interaction which is not needed for this study. For nearly all of these interactions, several estimates have been reported, and so for conciseness, only a range encompassing the most refined estimates is given here along with selected references: $B_{S/AN} = 6.7-8.0$,[47−50] $B_{S/MA} = 10.6-10.7$,[24,47] $B_{S/MMA} = 0.18-0.26$,[47,51−53] $B_{MMA/AN} = 4.1-4.5$[49,53,54]; and for MMA/MA a single report gives $B_{MMA/MA} = 7.18$[47] cal/cm^3. Without exception, these estimates were made by the analysis of copolymer blend phase behavior.

The predicted phase boundaries included in Figure 10 were calculated by choosing one set of binary interaction energies that simultaneously produced the best possible fit to each miscibility map. During the fitting process, the previously established interactions were subjected to the criteria that their values must fall within the ranges delimited above. The final set of binary interaction energies used in Figure 10 are summarized in Table 7. Included in the table are the average $B_{critical}$ values assumed for the calculations. With only a few exceptions, the predicted phase boundaries agree accurately with the experimental phase behavior. The discrepancies that do exist, for the most part, are for copolymers containing the highest amounts of either PMI or TBPMI. In these blends, lower than average molecular weights may contribute to the larger than predicted regions of miscibility. Taking the latter into account improves the quality of the predictions. Unfortunately, the unavailability of SMA copolymers containing between 35 and 45 wt % MA leaves a small gap in the respective miscibility maps, but this did not severely detract from the quality of the final analysis.

In addition to verifying and perhaps refining previously determined interaction energy estimates, Table 7 reports the first estimates for the binary interactions of PMI and TBPMI with S, AN, and MA. In all cases, the interactions are endothermic, becoming increasingly so going from styrene to acrylonitrile to maleic anhydride. The styrene interaction is more favorable with the brominated phenyl maleimide than with the phenyl maleimide; $B_{S/PMI} = 1.7 \pm 0.2 > B_{S/TBPMI} = 0.75 \pm 0.1$ cal/cm^3. The same trend was noted for PC where $B_{PC/PMI} = 1.0 \pm 0.15 > B_{PC/TBPMI} = 0.5 \pm 0.05$ cal/cm^3. While the trend is the same for MMA, $B_{MMA/PMI} = 1.0 \pm 0.1 > B_{MMA/TBPMI} = 0.8 \pm 0.05$ cal/cm^3, it is considerably less pronounced. With AN, the opposite trend exists where the addition of bromine actually makes the interaction more unfavorable; $B_{AN/PMI} = 2.0 \pm 0.5 < B_{AN/TBPMI} = 4.0 \pm 0.5$ cal/cm^3. The interactions with MA, $B_{MA/PMI} = 5.6 \pm 1.0$ and $B_{MA/TBPMI} = 5.8 \pm 1.0$ cal/cm^3, do not show an identifiable trend. In regard to the relatively large uncertainties assigned to the interactions with MA and AN above, these are not a reflection of the quality of the data or of the fit of the model to the data; rather, they are necessary to account for model being rather insensitive to these particular binary interaction energy values.

Explanations for the differences in brominated versus nonbrominated interactions can be postulated. Bromine atoms in tribromophenyl maleimide inductively withdraw electrons from the aromatic ring, leaving its center with larger, partial positive charge as compared to the nonbrominated phenyl maleimide. Ignoring steric differences between PMI and TBPMI, the delocalization of the electron density of the brominated aromatic ring could possibly allow more favorable interactions with the electron dense aromatic rings in PS and PC. This effect would not be present with PMMA because of the absence of aromatic rings. A second explanation could

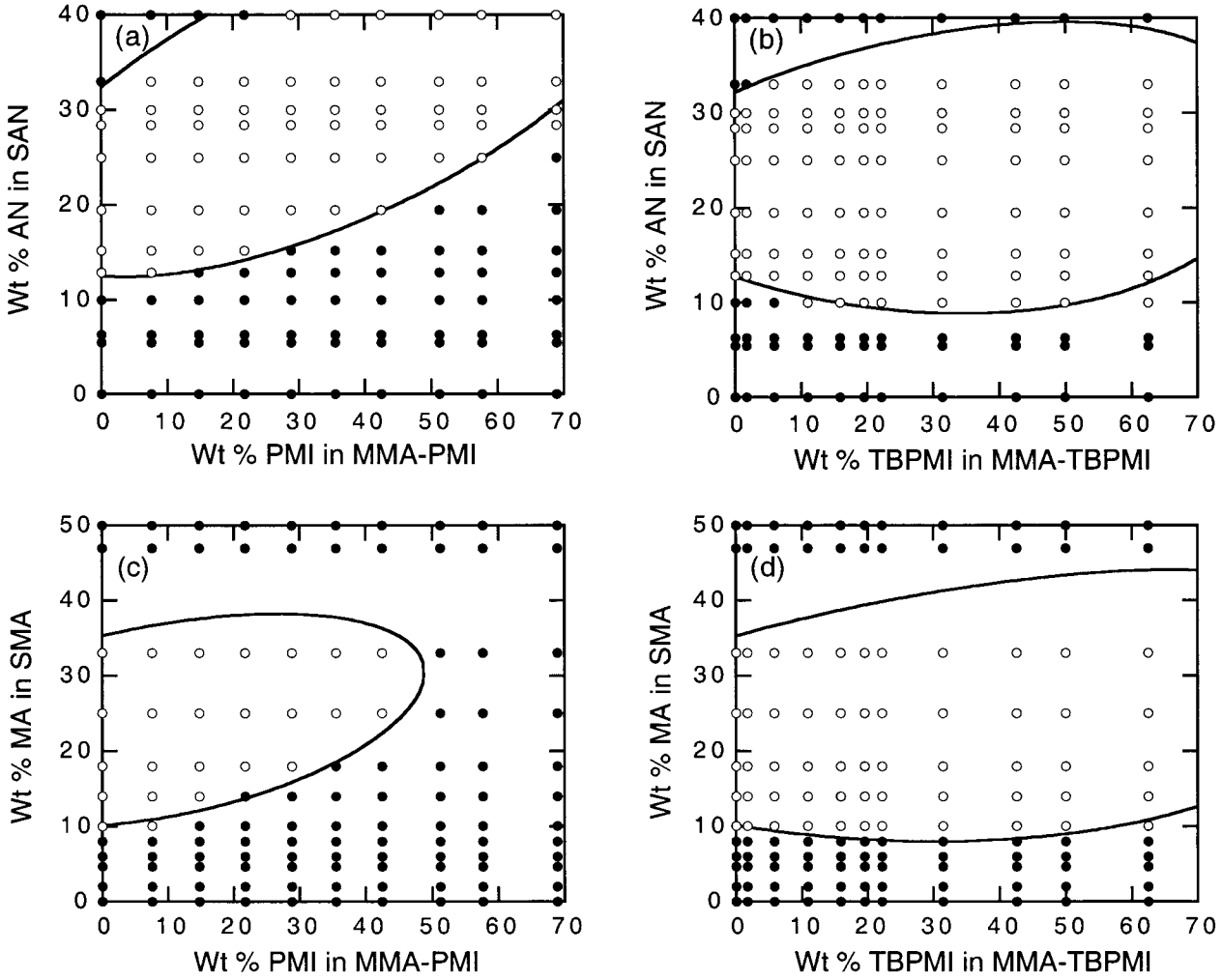

Figure 10. Isothermal miscibility maps measured at 170 °C for blends of SAN copolymers with (a) MMA−PMI and (b) MMA−TBPMI copolymers and for blends of SMA copolymers with (c) MMA−PMI and (d) MMA−TBPMI copolymers. Simultaneously optimizing the fit of the binary interaction modeled to all four plots allowed evaluation of the set of parameters listed in Table 7.

Table 7. Binary Interactions in B_{ij} in cal/cm^3 Used To Fit Data in Figure 8

	blend system			
binary pair	SAN/ MMA−PMI	SAN/ MMA−TBPMI	SMA/ MMA−PMI	SMA/ MMA−TBPMI
S/MMA	0.25	0.25	0.25	0.25
S/AN	6.9	6.9		
S/MA			10.6	10.6
S/PMI	1.7		1.7	
S/TBPMI		0.75		0.75
MMA/AN	4.3	4.3		
MMA/MA			7.0	7.0
MMA/PMI	1.1		1.1	
MMA/TBPMI		0.8		0.8
AN/PMI	2.0			
AN/TBPMI		4.0		
MA/PMI			5.6	
MA/TBPMI				5.8
$B_{critical}$	0.019	0.016	0.017	0.017

address the large decrease in the AN interaction with bromine substitution. The ortho-substituted bromines on the phenyl ring in TBPMI would likely sterically inhibit any close associations with the maleimide carbonyl dipoles, thus prohibiting interactions with the polar cyano groups in acrylonitrile. Both of the explanations proposed here are based on the presence of specific interactions. A noted precept of the binary interaction model used in this work, however, is that the interactions cannot be highly specific. Nonetheless, it has been demonstrated before that there is some latitude in applying this model as long as the energetic interactions do not severely compromise the random mixing approximation. Judging from the magnitude of the endothermic interaction energies evaluated here, application of the binary interaction model is justified.

Table 8. Summary of Binary Interaction Energies (cal/cm^3) Determined in This Study

binary pair	B_{ij}	eval temp (°C)	binary pair	B_{ij}	eval temp (°C)
MMA/PMI	1.0 ± 0.1	150	AN/PMI	2.0 ± 0.5	170
MMA/TBPMI	0.8 ± 0.05	150	AN/TBPMI	4.0 ± 0.5	170
PC/PMI	1.0 ± 0.15	150	MA/PMI	5.6 ± 1.0	170
PC/TBPMI	0.5 ± 0.05	240	MA/TBPMI	5.8 ± 1.0	170
S/PMI	1.7 ± 0.2	170	PMI/TBPMI	0.35 ± 0.05	150
S/TBPMI	0.75 ± 0.1	170			

Conclusions

The synthesis of MMA−PMI and MMA−TBPMI copolymers, their physical properties, and their blend phase behavior have been reported. Using the Flory−Huggins theory combined with a binary interaction model, the interaction energies of both PMI and TBPMI with MMA, PC, S, AN, MA and with each other were evaluated. A summary of these values are compiled in Table 8 which includes estimates of how precisely the values are known as well as the temperature at which

they were evaluated. In all cases, the interactions are highly endothermic, and for the most part, those with the brominated phenyl maleimide were more favorable than with the nonbrominated analogue. The clear exception is with AN where the opposite is found. Although the interactions are unfavorable, their incorporation into the MMA copolymers can actually enhance miscibility, as was shown here with PC. Composition-dependent regions of miscibility were also found with PMMA and with SAN and SMA copolymers. Attempts to predict phase separation temperatures for the miscible blends with PC by an equation-of-state approach yielded estimates that captured trends but not the magnitude of the experimentally measured values.

Acknowledgment. Financial support for this work was provided by the National Science Foundation (Grants DMR 92-15926 and DMR 97-26484), administered by the Division of Materials Research−Polymers Program.

References and Notes

(1) Fire, F. L. *Combustibility of Plastics*; van Nostrand Reinhold: New York, 1991.
(2) Troitzsch, J. *Makromol. Chem., Macromol. Symp.* **1993**, *74*, 125.
(3) Wigotsky, V. *Plast. Eng.* **July 1997**, 20.
(4) Woo, E. M.; Barlow, J. W.; Paul, D. R. *J. Appl. Polym. Sci.* **1983**, *28*, 1347.
(5) Woo, E. M.; Barlow, J. W.; Paul, D. R. *J. Polym. Sci., Polym. Symp.* **1984**, *71*, 137.
(6) Woo, E. M.; Barlow, J. W.; Paul, D. R. *J. Appl. Polym. Sci.* **1985**, *30*, 4243.
(7) Woo, E. M.; Barlow, J. W.; Paul, D. R. *Polymer* **1985**, *26*, 763.
(8) Woo, E. M.; Barlow, J. W.; Paul, D. R. *J. Appl. Polym. Sci.* **1986**, *32*, 3889.
(9) Fernandes, A. C.; Barlow, J. W.; Paul, D. R. *J. Appl. Polym. Sci.* **1984**, *29*, 1971.
(10) Fernandes, A. C.; Barlow, J. W.; Paul, D. R. *J. Appl. Polym. Sci.* **1986**, *32*, 5481.
(11) Fernandes, A. C.; Barlow, J. W.; Paul, D. R. *J. Appl. Polym. Sci.* **1986**, *32*, 6073.
(12) Kim, C. K.; Paul, D. R. *Polymer* **1992**, *33*, 4929.
(13) Flory, P. J. *J. Chem. Phys.* **1942**, *10*, 51.
(14) Huggins, M. L. *J. Chem. Phys.* **1941**, *9*, 440.
(15) Koningsveld, R.; Chermin, H. A. G. *Proc. R. Soc. London A* **1970**, *319*, 331.
(16) Koningsveld, R.; Kleintjens, L. A. *J. Polym. Sci., Polym. Symp.* **1977**, *61*, 221.
(17) Kambour, R. P.; Bendler, J. T.; Bopp, R. C. *Macromolecules* **1983**, *16*, 753.
(18) ten Brinke, G.; Karasz, F. E.; MacKnight, W. J. *Macromolecules* **1983**, *16*, 1827.
(19) Paul, D. R.; Barlow, J. W. *Polymer* **1984**, *25*, 487.
(20) Sanchez, I. C.; Lacombe, R. H. *Macromolecules* **1978**, *11*, 1145.
(21) Sanchez, I. C. Polymer Phase Separation. In *Encyclopedia of Physical Science and Technology*; Meyers, R. A., Ed.; Academic Press: New York, 1992; Vol. 13.
(22) Sanchez, I. C.; Panayiotou, C. G. In *Models of Thermodynamic and Phase Equilibrium Calculations*; Sandler, S. I., Ed.; Marcel Dekker: New York, 1994; Chapter 3.
(23) Callaghan, T. A. Ph.D. Dissertation, The University of Texas at Austin, 1992.
(24) Merfeld, G. D.; Paul, D. R. *Polymer* **1998**, *39*, 1999.
(25) Janovic, Z.; Matusinovic, T. T. *Makromol. Chem.* **1993**, *194*, 1915.
(26) Janovic, Z.; Malavasic, T.; Saric, K. *Macromol. Chem., Macromol. Symp.* **1993**, *74*, 277.
(27) Janovic, Z. *Macromol. Symp.* **1995**, *100*, 89.
(28) Bharel, R.; Choudhary, V.; Varma, I. K. *J. Appl. Polym. Sci.* **1993**, *49*, 31.
(29) Choudhary, L.; Varma, D. S.; Varma, I. K.; Wang, F. W. *J. Therm. Anal.* **1993**, *39*, 633.
(30) Barrales-Rienda, J. M.; Gonzalez de la Campa, J. I.; Gonzalez Ramos, J. *J. Macromol. Sci.-Chem.* **1977**, *A11*, 267.
(31) Kumar, A. *J. Macromol. Sci.* **1987**, *A24*, 711.
(32) Merfeld, G. D. Ph.D. Dissertation, The Univeristy of Texas at Austin, 1998.
(33) Kim, C. K.; Paul, D. R. *Polymer* **1992**, *33*, 1630.
(34) Nishimoto, M.; Keskkula, H.; Paul, D. R. *Polymer* **1991**, *32*, 1274.
(35) Ohnaga, T.; Sato, T.; Nagata, S. *Polymer* **1997**, *38*, 1073.
(36) Dean, B. D. US Patent No. 4,491,647, 1985 (Atlantic Richfield Co.).
(37) Dean, B. D.; Le-Khac, B. US Patent No. 4,749,746, 1988 (Arco Chemical Co.).
(38) Ikawa, K.; Hosoda, S. *Polym. Networks Blends* **1991**, *1*, 103.
(39) Callaghan, T. A.; Paul, D. R. *J. Polym. Sci., Part B: Polym. Phys.* **1994**, *32*, 1813.
(40) Dean, B. D. *J. Appl. Polym. Sci.* **1985**, *30*, 4193.
(41) Dean, B. D. US Patent No. 4,504,627, 1985 (Atlantic Richfield Co.).
(42) Dean, B. D. US Patent No. 4,514,543, 1985 (Atlantic Richfield Co.).
(43) Dean, B. D. US Patent No. 4,720,525, 1988 (Atlantic Richfield Co.).
(44) Fowler, M. E.; Barlow, J. W.; Paul, D. R. *Polymer* **1987**, *28*, 1177.
(45) Kim, J. H.; Barlow, J. W.; Paul, D. R. *J. Polym. Sci., Part B: Polym. Phys.* **1989**, *27*, 223.
(46) Brannock, G. R.; Barlow, J. W.; Paul, D. R. *J. Polym. Sci., Part B: Polym. Phys.* **1991**, *29*, 413.
(47) Gan, P. P.; Paul, D. R. *J. Appl. Polym. Sci.* **1994**, *54*, 317.
(48) Keitz, J. D.; Barlow, J. W.; Paul, D. R. *J. Appl. Polym. Sci.* **1984**, *29*, 3131.
(49) Nishimoto, M.; Keskkula, H.; Paul, D. R. *Polymer* **1989**, *30*, 1279.
(50) Nishimoto, M.; Keskkula, H.; Paul, D. R. *Macromolecules* **1990**, *23*, 3633.
(51) Fukuda, T.; Nagata, M.; Inagaki, H. *Macromolecules* **1986**, *19*, 1411.
(52) Callaghan, T. A.; Paul, D. R. *Macromolecules* **1993**, *26*, 2439.
(53) Gan, P. P.; Padwa, A. R.; Paul, D. R. *Polymer* **1994**, *35*, 1487.
(54) Chu, J.; Paul, D. R. Submitted to Polymer.

MA981230P